Journal of Alloys and Compounds 509 (2011) 5858–5862

Contents lists available at ScienceDirect

Journal of Alloys and Compounds

journal homepage: www.elsevier.com/locate/jallcom

Phase transition and electrical properties of $(1-x)K_{0.02}Na_{0.98}NbO_3$–$xBaTiO_3$ ceramics

Jiangtao Zeng[a,*], Liaoying Zheng[a], Guorong Li[a], Zhenzhu Cao[a], Kunyu Zhao[a], Qingrui Yin[a], Ekaterina D. Politova[b]

[a] Key Laboratory of Inorganic Functional Materials and Devices, Shanghai Institute of Ceramics, Chinese Academy of Sciences, Shanghai 200050, PR China
[b] L. Ya. Karpov Institute of Physical Chemistry, Obukha Side-Str. 3-1/12, b. 6, Moscow 105064, Russia

ARTICLE INFO

Article history:
Received 29 August 2010
Received in revised form 24 February 2011
Accepted 25 February 2011
Available online 5 March 2011

Keywords:
Ceramics
Ferroelectrics
Piezoelectricity
Phase transitions
Dielectric response

ABSTRACT

$(1-x)K_{0.02}Na_{0.98}NbO_3$–$xBaTiO_3$ ceramics were prepared by the solid state reaction method, and their electrical properties were investigated. The samples showed crystal structure changing from monoclinic to orthorhombic, and then to tetragonal, with an increase in $BaTiO_3$ content. The addition of $BaTiO_3$ markedly enhanced ferroelectric and piezoelectric properties of $K_{0.02}Na_{0.98}NbO_3$ ceramics. Remnant polarization increased and coercive field decreased only in the samples with small amount of $BaTiO_3$. Piezoelectric properties were improved with the addition of $BaTiO_3$. The $0.9K_{0.02}Na_{0.98}NbO_3$–$0.1BaTiO_3$ ceramics showed maximum piezoelectric constant (d_{33} = 160 pC/N), which was even comparable with that of $(1-x)K_{0.5}Na_{0.5}NbO_3$–$xBaTiO_3$ ceramics. Their good piezoelectric properties, along with a low ferroelectric–ferroelectric transition temperature (T_{F-F}), made the $0.9K_{0.02}Na_{0.98}NbO_3$–$0.1BaTiO_3$ ceramics a potential candidate for lead-free piezoelectric applications.

1. Introduction

Potassium sodium niobate [(K, Na)NbO_3, KNN] based ceramics have been intensively studied from the point view of environmental protection. KNN-based ceramics have high Curie temperature and high piezoelectric properties, which are even comparable with those of PZT-based ceramics. As a result, they are the most promising candidates as lead-free piezoelectric ceramics [1–3].

Pure KNN ceramics have rather low piezoelectric properties. Different dopants are studied to improve their piezoelectric properties, including Li^+, Ta^{5+}, Sb^{5+}, $Bi(Zn_{0.5}Ti_{0.5})O_3$, $BaTiO_3$, etc. [4–8]. $BaTiO_3$ modified $K_{0.5}Na_{0.5}NbO_3$ ceramics were studied by many researchers. Piezoelectric properties of the $K_{0.5}Na_{0.5}NbO_3$–$BaTiO_3$ ceramics prepared by the conventional sintering method were improved, with piezoelectric constant being not very high (d_{33} = 104 pC/N) [7]. Comparatively, $K_{0.5}Na_{0.5}NbO_3$–$BaTiO_3$ ceramics fabricated by the hot pressing method had enhanced piezoelectric constant (d_{33} = 225 pC/N) [8]. It means that the piezoelectric properties of $K_{0.5}Na_{0.5}NbO_3$–$BaTiO_3$ ceramics are strongly dependent on processing. Another challenge for KNN ceramics is how to get dense ceramics. Different methods are studied to improve the sinterability of $K_{0.5}Na_{0.5}NbO_3$ ceramics, including powder processing [9], pressure sintering [10], and the addition of sintering aids [11,12]. It is believed that the high moisture sensitivity of K_2CO_3 and the volatilization of K_2O are the main cause of the poor sinterability of KNN ceramics. Therefore, it is expected that KNN ceramics with low content of K could have better sinterability. Unfortunately KNN ceramics with low potassium concentration have rarely been studied.

In this paper, dielectric and piezoelectric properties of $BaTiO_3$ doped $K_{0.02}Na_{0.98}NbO_3$ ceramics were studied. The doped K2NN ceramics demonstrated markedly enhanced piezoelectric properties.

2. Experimental

$(1-x)K_{0.02}Na_{0.98}NbO_3$–$xBaTiO_3$ ceramics with x = 0.00, 0.05, 0.07, 0.08, 0.10, 0.12, 0.14 (K2NNBT100x), were prepared by the solid-state reaction method. Raw materials used, Na_2CO_3, K_2CO_3, $BaCO_3$ and Nb_2O_5, are all of high purity. The raw materials in stoichiometric ratios of the compositions were mixed thoroughly in ethanol by ball-milling for 8 h and then dried and calcined at 900 °C for 2 h in an alumina crucible. After calcination, the mixtures were ground and ball-milled again. The milled powders were pressed into disks 2 mm thick with diameters of 12 mm. The disk samples were finally sintered at 1200–1300 °C for 2 h in ambient atmosphere. Silver electrodes were fired on top and bottom surfaces of the samples for subsequent electrical measurement.

Bulk densities of the sintered ceramics were measured by the Archimedes method. Crystal structure of the sintered samples was studied by using X-ray diffraction (XRD) analysis with Cu Kα radiation (D/max 2550 V). Microstructures of polished surfaces of the K2NNBT100x ceramics were examined by using SEM (KYKY-EM3200). All the samples were thermally etched before SEM examination. Dielectric constant ε and loss tan δ at 1 kHz, 10 kHz and 100 kHz of the ceramics were measured as a function of temperature by using a LCR meter (Agilent 4294A).

* Corresponding author. Tel.: +86 21 52412034; fax: +86 21 52413122.
E-mail address: zjt@mail.sic.ac.cn (J. Zeng).

0925-8388/$ – see front matter © 2011 Elsevier B.V. All rights reserved.
doi:10.1016/j.jallcom.2011.02.152

A conventional Sawyer–Tower circuit was used to measure the polarization–electric field (P–E) hysteresis loop at room temperature. Piezoelectric charge coefficient d_{33} was measured by using a piezo d_{33} meter (ZJ-3A, Institute of Acoustics, Chinese Academy of Sciences). Electromechanical coupling coefficient k_p was determined using the IEEE Std. 176 method from the impedance data measured by using an impedance analyzer (Agilent 4294A). Prior to the d_{33} and k measurements, the ceramics were poled at a DC field of 40–60 kV/cm at 80–120 °C in a silicone oil bath for 30 min.

3. Results and discussion

K2NNBT100x showed very good sinterability. All samples had relative density of above 95%. $BaTiO_3$ doping slightly decreased the optimum sintering temperature from 1300 °C for K2NN to 1220 °C for K2NNBT14.

Fig. 1 shows XRD patterns of K2NNBT100x ceramics. All ceramics were single phase perovskite structure and no secondary phases were detected. K2NN ceramics structure is slightly monoclinically distorted with $\beta = 90.53°$, which is close to the value in PCPDF Card No. 74-2024. $BaTiO_3$ doping changed crystal structure markedly, which was evidenced by the change in the 2θ reflection peak near 32° (shown in Fig. 2b). For K2NN, the 2θ peak near 32° can be fitted to 3 peaks by Lorentzian fit, while for K2NNBT5 the peak can be fitted to 2 peaks and there is only one peak for K2NNBT10 ceramics. It means that K2NN ceramics is monoclinic, while K2NNBT100x are orthorhombic at $0.05 \leq x \leq 0.08$ and tetragonal at $0.10 \leq x \leq 0.14$. There are two polymorphic phase transitions (PPT) in K2NNBT100x: monoclinic–orthorhombic phase transition at $x = 0$–0.05 and orthorhombic–tetragonal phase transition at $x = 0.08$–0.10.

Fig. 2 shows SEM micrographs of the K2NN, K2NNBT5, K2NNBT10 and K2NNBT12 ceramics sintered at their optimized temperatures (1300 °C for K2NN, 1280 °C for K2NNBT5, 1240 °C for K2NNBT10 and K2NNBT12). K2NN ceramics sintered at 1300 °C have rather large grains (4–6 μm). For K2NNBT5 ceramics, the optimum sintering temperature decreased by 20 °C, and the grain size is much smaller than that of K2NN ceramics. K2NNBT10 and K2NNBT12 ceramics were sintered at the same temperature, but the grain size of K2NNBT5 ceramics is larger than that of K2NNBT10 ceramics. It indicates that the addition of $BaTiO_3$ could facilitate the grain growth of K2NNBT100x ceramics.

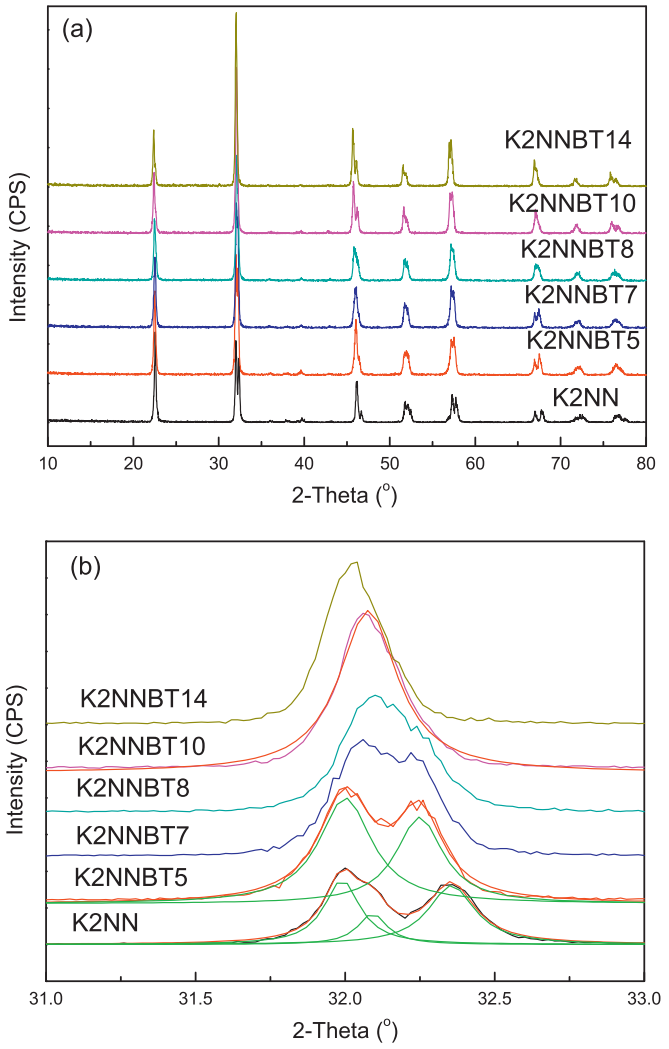

Fig. 1. (a) XRD patterns of the K2NNBT100x ceramics; (b) enlarged XRD patterns of the K2NNBT100x ceramics and Lorentzian fitting of the patterns.

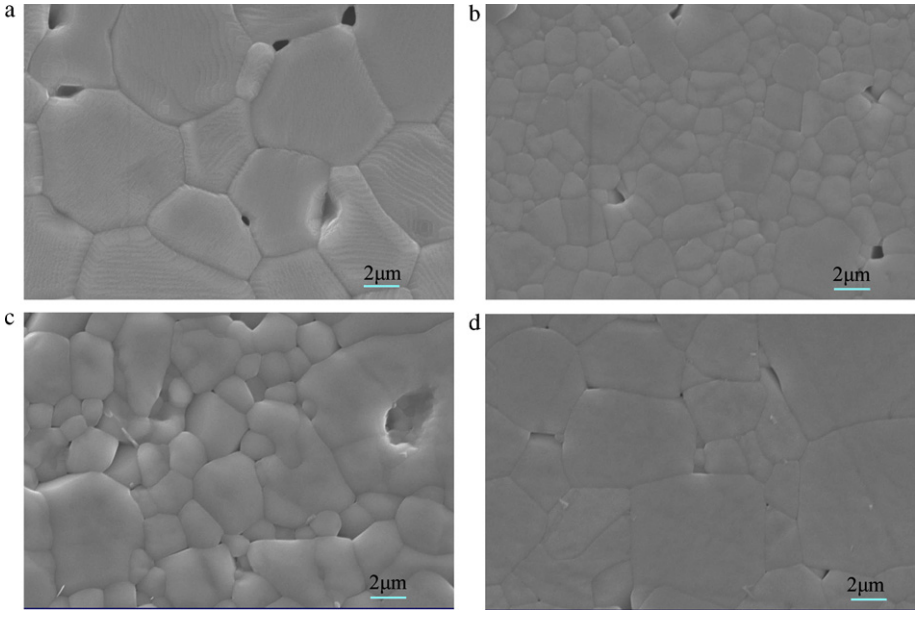

Fig. 2. SEM micrographs of K2NNBTx ceramics sintered at their optimal temperatures (1300 °C for K2NN, 1280 °C for K2NNBT5, 1240 °C for K2NNBT10 and K2NNBT12): (a) K2NN; (b) K2NNBT5; (c) K2NNBT10; (d) K2NNBT12.

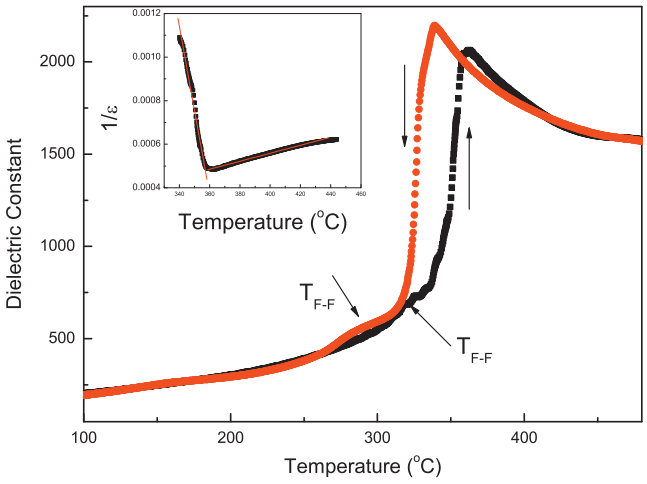

Fig. 3. Temperature dependence of dielectric constant of the K2NN ceramics (1 kHz) measured at heating and cooling. The inset shows inverse dielectric constant below and above Curie temperature.

Fig. 3 shows the temperature dependence of the dielectric constant of K2NN ceramics (1 kHz) measured during heating and cooling. With increasing temperature, KNN reveals a phase transition from ferroelectric to paraelectric phase at 365 °C. There is another small anomaly just below the Curie temperature. When cooling from high temperature, the dielectric constant peak appears at lower temperature. The thermal hysteresis indicates that the phase transition is the first-order one. The dielectric anomaly below the Curie temperature can be seen more clearly when cooling from high temperature. This dielectric anomaly should be caused by a ferroelectric–ferroelectric phase transition. Unlike phase transition in $K_{0.5}Na_{0.5}NbO_3$ ceramics, the ferroelectric–ferroelectric transition of K2NN is not so obvious and the transition temperature (T_{F-F}) is very close to the ferroelectric–paraelectric phase transition temperature. Inverse of the dielectric constant below and above the Curie temperature is shown as inset in Fig. 3. It follows the Curie–Weiss law, but the ratio of the slopes below and above T_C is about 36. In traditional theory, the ratio for the first order phase transition should be close to 8 [13]. In some ceramics, intermediate phase between ferroelectric and paraelectric ones could have similar phenomena [14].

Fig. 4 shows temperature dependence of dielectric constant of the K2NNBT100*x* ceramics. The addition of $BaTiO_3$ greatly changed the dielectric behavior of K2NN. Although the maximum dielectric constant at the Curie temperature (ε_m) for K2NN is quite low, ε_m increased markedly with increasing $BaTiO_3$ content. K2NNBT10 ceramics has the largest ε_m (>10,000) which is even higher than that of doped $K_{0.5}Na_{0.5}NbO_3$ ceramics [4,5]. Fig. 4b shows low temperature range data of Fig. 4a. It can be seen that the ferroelectric–ferroelectric phase transition is more pronounced as compared to the undoped ceramics. Phase transition shifts to low temperature with increasing $BaTiO_3$ content. The variations in T_C and T_{F-F} with x are shown in Fig. 5. T_{F-F} decreases linearly with increasing x according to the equation:

$$T_{F-F} = 327.4 - 3423.7x \quad (1)$$

It can be estimated that T_{F-F} is −15 °C at $x = 0.10$. Low T_{F-F} is crucial to afford temperature stability of piezoelectric properties for KNN based ceramics [15]. T_C of the K2NNBT100*x* ceramics also decreases with increasing x. T_C decreases linearly at $x \geq 0.05$, but it is not the case at lower x, indicating that the ferroelectric–paraelectric phased transition at $x = 0$ is different from those of samples with other compositions. Fig. 6 shows dielectric loss plotted versus temperature of the K2NNBT100*x* ceramics (1 kHz). All samples have

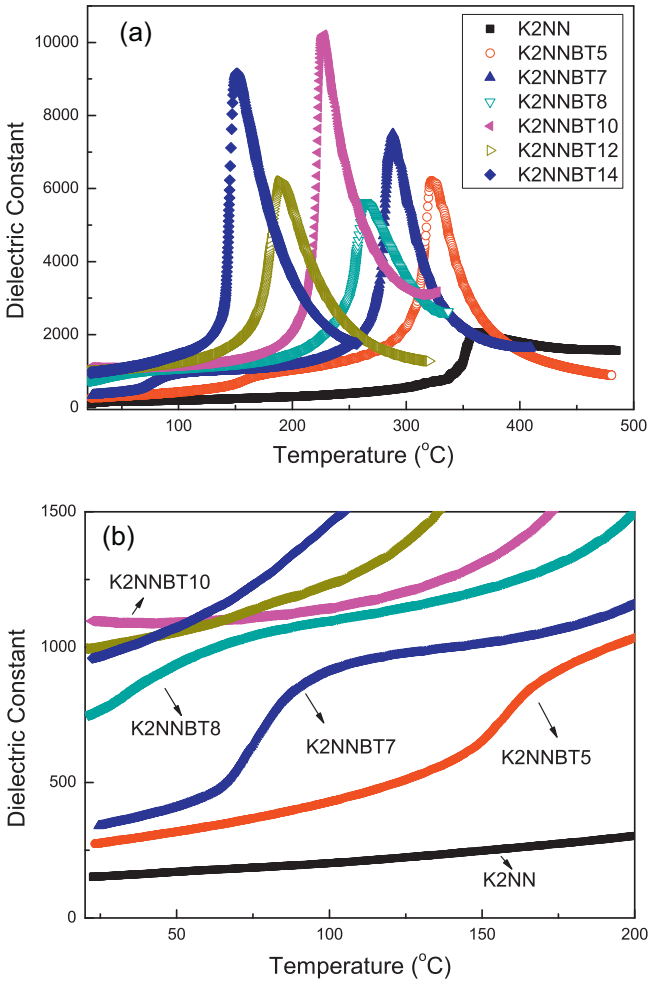

Fig. 4. (a) Temperature dependence of dielectric constant of the K2NNBT100*x* ceramics (1 kHz); (b) low temperature range of (a).

dielectric loss less than 0.1 at temperatures below T_C. It increases rapidly above T_C.

Fig. 7a shows *P*–*E* hysteresis loops of the k2NNBT100*x* ceramics. All loops are well saturated. As for K2NN ceramics, it is difficult to get a saturated loop at room temperature, so the measurements were taken at 100 °C. The variations in remnant polarization Pr and coercive field Ec are shown as Fig. 7b. The K2NN ceramics has

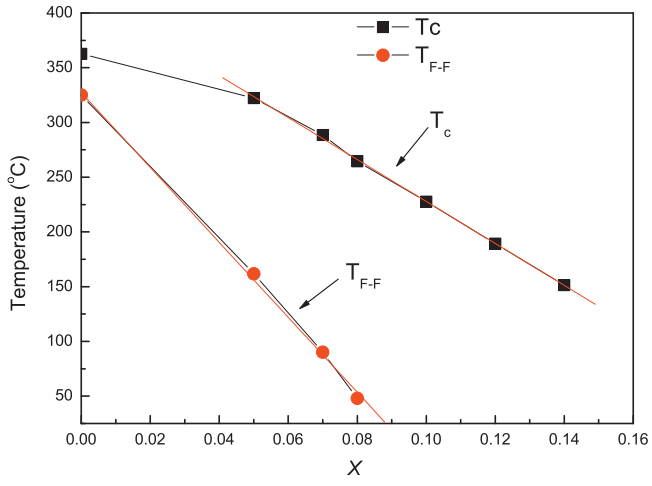

Fig. 5. T_C and T_{F-F} of the K2NNBT100*x* ceramics plotted versus *x*.

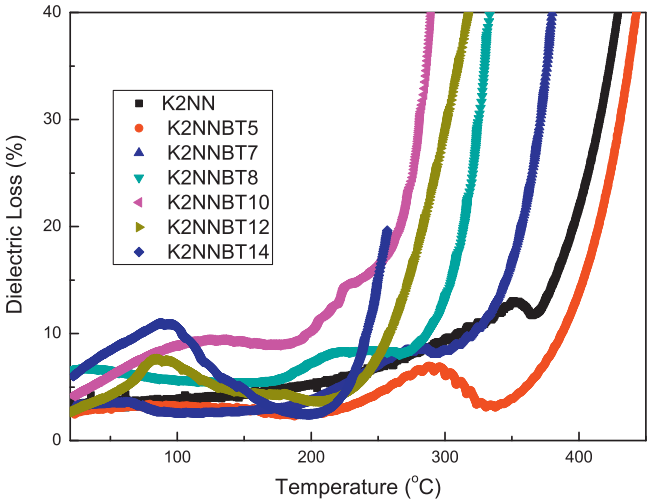

Fig. 6. Temperature dependence of dielectric loss of the K2NNBT100*x* ceramics (1 kHz).

small Pr, but high Ec values. With increasing $BaTiO_3$ content, the Pr value of K2NNBT100*x* increases at first and then decreases. It reaches maximum at $x = 0.08$. Ec decreases rapidly with increasing x at $x \leq 0.07$. The large Pr and low Ec values of the K2NNBT8 ceramics also indicate that there exists a PPT at about $x = 0.08$–0.1.

Fig. 8 shows piezoelectric constant d_{33} and electromechanical coefficient k_p plotted versus x. The K2NN ceramics has very low d_{33} (44 pC/N) and small k_p due to the small Pr and high Ec. With increasing BT, first d_{33} increases slightly, and then increases rapidly near the phase boundary, reaching the maximum at $x = 0.10$. d_{33} and k_p decrease with further increase in the BT content. For K2NNBT10, d_{33} is 160 pC/N and k_p is 0.34. Piezoelectric constant d_{33} of the K2NNBT10 ceramics increases by 260% as compared to that of K2NN ceramics. It should be noted that this value is very close to that of the $K_{0.5}Na_{0.5}NbO_3$–$BaTiO_3$ system, though the piezoelectric properties of K2NN are much worse than those of $K_{0.5}Na_{0.5}NbO_3$ [7,8]. Taking into account its low T_{F-F} value, K2NNBT10 should be regarded as promising lead-free ceramics for practical applications. The enhanced piezoelectric properties of the K2NNBT10 ceramics revealed may be attributed to their large Pr and low Ec values.

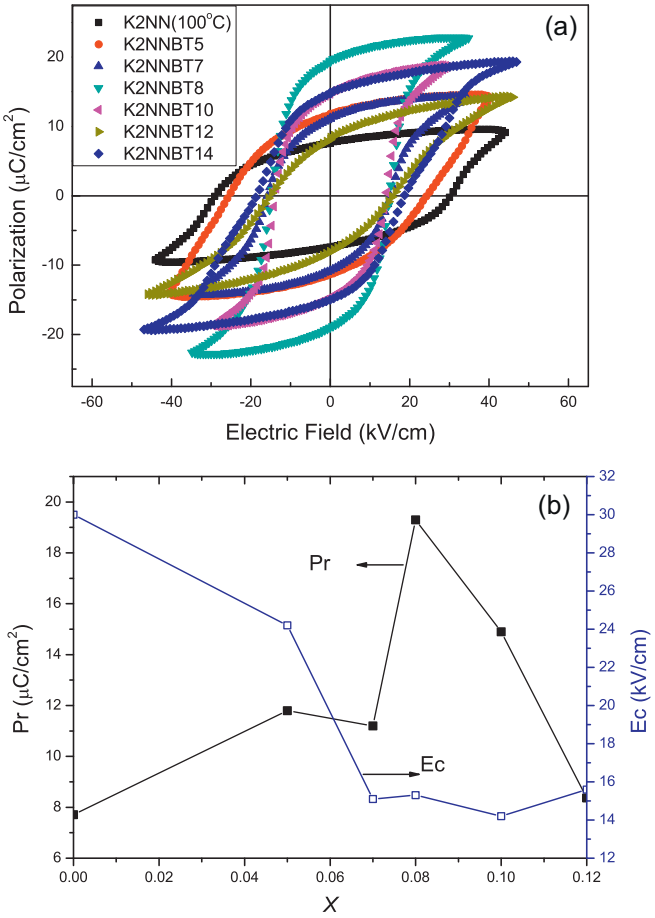

Fig. 7. (a) *P*–*E* hysteresis loops of the K2NNBT100*x* ceramics; (b) variation of Pr and Ec of the K2NNBT100*x* ceramics with *x*.

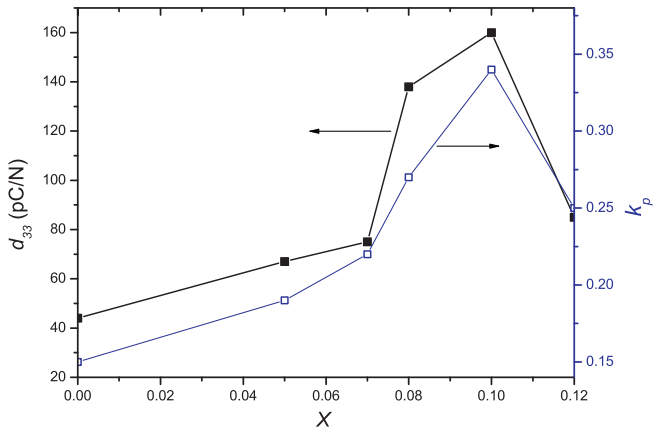

Fig. 8. Variation of piezoelectric constant d_{33} and electromechanical coefficient k_p of the k2NNBT100*x* ceramics plotted versus *x*.

4. Conclusions

$(1-x)K_{0.02}Na_{0.98}NbO_3$–$xBaTiO_3$ ceramics were prepared by the solid state reaction method. Their crystal structures changed from monoclinic to orthorhombic, then to tetragonal with increasing $BaTiO_3$ content. The phase boundary between orthorhombic structure and tetragonal structure is situated at $x = 0.08$–0.10. Addition of $BaTiO_3$ markedly enhanced ferroelectric and piezoelectric properties of $K_{0.02}Na_{0.98}NbO_3$ ceramics. Remnant polarization increased and coercive field decreased with an increase in $BaTiO_3$ content first. With excessive addition of $BaTiO_3$, remnant polarization decreased while coercive field slightly increased. Piezoelectric properties were also improved if small amount of $BaTiO_3$ was added. The $0.9\,K_{0.02}Na_{0.98}NbO_3$–$0.1BaTiO_3$ ceramics showed very promising piezoelectric properties, which were comparable with those of $(1-x)K_{0.5}Na_{0.5}NbO_3$–$xBaTiO_3$ ceramics. These ceramics also had low ferroelectric–ferroelectric phase transition temperature that means that they have high thermal stability in piezoelectric properties. This study has proved that it is possible to develop high performance KNN ceramics by using compositions other than $K_{0.5}Na_{0.5}O_3$.

Acknowledgements

This work was supported by the Ministry of Sciences and Technology of China through 973-project (No. 2009CB623305), and Natural Science Foundation of China (Nos.: 50702068, 50977088, 51011120098).

References

[1] Y. Saito, H. Takao, I. Tani, T. Nonoyama, K. Takatori, T. Homma, T. Nagaya, M. Nakamura, Nature 432 (2004) 84–87.

[2] B.Q. Ming, J.F. Wang, P. Qi, G.Z. Zang, J. Appl. Phys. 101 (2007) 054103–054106.
[3] K. Wang, J.F. Li, Adv. Funct. Mater. 20 (2010) 1924–1929.
[4] D. Lin, K.W. Kwok, H.L. Chan, J. Am. Ceram. Soc. 92 (2009) 2765–2767.
[5] Z.Y. Shen, Y.H. Zhen, K. Wang, J.F. Li, J. Am. Ceram. Soc. 92 (2009) 1748–1752.
[6] M. Sutapun, C.C. Huang, D.P. Cann, N. Vittayakorn, J. Alloys Compd. 479 (2009) 462–466.
[7] Y.P. Guo, K.-I. Kakimoto, H. Ohsato, Jpn. J. Appl. Phys. 43 (2004) 6662–6666.
[8] H. Park, C. Ahn, H. Song, J. Lee, S. Nahma, K. Uchino, H. Lee, H. Lee, Appl. Phys. Lett. 89 (2006) 062906–062909.
[9] K.C. Singh, C. Jiten, R. Laishram, O.P. Thakur, D.K. Bhattachary, J. Alloys Compd. 496 (2010) 717–722.
[10] R. López-Juáreza, F. González-Garcíab, J. Zárate-Medinac, R. Escalona-Gonzálezd, S.D. Torred, M.E. Villafuerte-Castrejón, J. Alloys Compd. 509 (2011) 3837–3842.
[11] J. Bernard, A. BenČan Wan, T. Rojac, J. Holc, B. MalČi, M. Kosec, J. Am. Ceram. Soc. 91 (2008) 2409–2411.
[12] X.P. Jiang, Q. Yang, Z.D. Yu, F. Hu, C. Chen, N. Tu, Y.M. Li, J. Alloys Compd. 493 (2010) 276–280.
[13] R. Waser, Polar Oxides: Properties, Characterization and Imaging, Wiley-VCH, Weinheim, 2005.
[14] B. Jaffe, W.R. Cook, H. Jaffe, Piezoelectric Ceramics, Academic Press, New York, 1971.
[15] H.L. Du, W.C. Zhou, F. Luo, D.M. Zhu, S.B. Qu, Z.B. Pei, Appl. Phys. Lett. 91 (2007) 182909–182911.